

Wave-equation inversion prestack Hessian

Alejandro A. Valenciano and Biondo Biondi

ABSTRACT

The angle-domain Hessian can be computed from the subsurface-offset domain Hessian by an offset-to-angle transformation. An understanding of how the seismic energy is distributed with reflection angle can be gained by explicitly computing the angle-domain Hessian. The Hessian computation in a model with a single reflector under a Gaussian velocity anomaly (creating uneven illumination) illustrates the theory.

INTRODUCTION

Seismic imaging using non-unitary migration operators (Claerbout, 1992) often produces images with reflectors correctly positioned but biased amplitudes (Nemeth et al., 1999; Duquet and Marfurt, 1999; Ronen and Liner, 2000; Chavent and Plessix, 1999). One way to solve this problem is to apply inversion theory (Tarantola, 1987), where the image can be obtained by convolving the migrated image with the inverse of the Hessian matrix. However, when the dimensions of the problem get large, the explicit calculation of the Hessian matrix and its inverse becomes unfeasible.

To reduce the size of the problem Valenciano and Biondi (2004) proposed to compute the Hessian in a target-oriented fashion. By explicitly computing the Hessian, the zero-offset inverse image can be obtained using an iterative inversion algorithm (Valenciano et al., 2005a,b). This approach renders unnecessary an explicit computation of inverse of the Hessian matrix.

In this paper we show an example of the computation of the wave-equation angle-domain Hessian. It was defined by Valenciano and Biondi (2005) via an offset-to-angle transformation (Fomel, 2004; Sava and Fomel, 2003). Since the angle-domain Hessian matrix is explicitly computed, a better understanding of the uneven illumination in complex subsurface scenarios can be gained. We illustrate our method by computing the Hessian for a model that contains one reflector under a Gaussian velocity anomaly which creates uneven illumination.

EXPANDING HESSIAN DIMENSIONALITY

Valenciano et al. (2005b) define the zero subsurface-offset domain Hessian by using the adjoint of the zero subsurface-offset domain migration as the modeling operator \mathbf{L} . Then the zero-

subsurface-offset inverse image can be estimated as the solution of a non-stationary least-squares filtering problem, using an iterative inversion algorithm (Valenciano et al., 2005a,b).

From the results reported by Prucha et al. (2000), Kuehl and Sacchi (2001), and Valenciano et al. (2005a), regularization in the reflection angle dimension is necessary to stabilize the wave-equation inversion problem. That is why Valenciano and Biondi (2005) defined the wave-equation angle-domain Hessian from the subsurface offset wave-equation Hessian via an angle-to-offset transformation (Fomel, 2004; Sava and Fomel, 2003).

The next subsections summarize the theory presented in (Valenciano et al., 2005b).

Subsurface-offset Hessian

The prestack migration image (subsurface offset domain) for a group of shots positioned at $\mathbf{x}_s = (x_s, y_s, 0)$ and a group of receivers positioned at $\mathbf{x}_r = (x_r, y_r, 0)$ can be given by the adjoint of a linear operator \mathbf{L} acting on the data-space $\mathbf{d}(\mathbf{x}_s, \mathbf{x}_r; \omega)$ as

$$\begin{aligned} \mathbf{m}(\mathbf{x}, \mathbf{h}) &= \mathbf{L}' \mathbf{d}(\mathbf{x}_s, \mathbf{x}_r; \omega) \\ &= \sum_{\omega} \sum_{\mathbf{x}_s} \sum_{\mathbf{x}_r} \mathbf{G}'(\mathbf{x} + \mathbf{h}, \mathbf{x}_s; \omega) \mathbf{G}'(\mathbf{x} - \mathbf{h}, \mathbf{x}_r; \omega) \sum'_{\mathbf{h}} \sum'_{\mathbf{x}} \mathbf{d}(\mathbf{x}_s, \mathbf{x}_r; \omega), \end{aligned} \quad (1)$$

where $\mathbf{G}(\mathbf{x}, \mathbf{x}_s; \omega)$ and $\mathbf{G}(\mathbf{x}, \mathbf{x}_r; \omega)$ are respectively the Green's functions from the shot position \mathbf{x}_s and from the receiver position \mathbf{x}_r to a point in the model space \mathbf{x} , and $\mathbf{h} = (h_x, h_y)$ is the subsurface offset. The symbols $\sum'_{\mathbf{h}}$ and $\sum'_{\mathbf{x}}$ are spray (adjoint of the sum) operators in the subsurface offset and model space dimensions, respectively. The Green's functions are computed by means of the one-way wave-equation.

The synthetic data can be modeled (as the adjoint of equation 1) by the linear operator \mathbf{L} acting on the model space $\mathbf{m}(\mathbf{x}, \mathbf{h})$ with $\mathbf{x} = (x, y, z)$ and $\mathbf{h} = (h_x, h_y)$

$$\begin{aligned} \mathbf{d}(\mathbf{x}_s, \mathbf{x}_r; \omega) &= \mathbf{Lm}(\mathbf{x}, \mathbf{h}) \\ &= \sum_{\mathbf{x}} \sum_{\mathbf{h}} \mathbf{G}(\mathbf{x} - \mathbf{h}, \mathbf{x}_r; \omega) \mathbf{G}(\mathbf{x} + \mathbf{h}, \mathbf{x}_s; \omega) \sum'_{\mathbf{x}_r} \sum'_{\mathbf{x}_s} \sum'_{\omega} \mathbf{m}(\mathbf{x}, \mathbf{h}), \end{aligned} \quad (2)$$

where the symbols $\sum'_{\mathbf{x}_r}$, $\sum'_{\mathbf{x}_s}$, and \sum'_{ω} are spray operators in the shot, receiver, and frequency dimensions, respectively.

The quadratic cost function is

$$S(\mathbf{m}) = \frac{1}{2} \sum_{\omega} \sum_{\mathbf{x}_s} \sum_{\mathbf{x}_r} \|\mathbf{d} - \mathbf{d}_{obs}\|^2, \quad (3)$$

and its second derivative with respect to the model parameters $\mathbf{m}(\mathbf{x}, \mathbf{h})$ and $\mathbf{m}(\mathbf{x}', \mathbf{h}')$ is the subsurface offset Hessian:

$$\mathbf{H}(\mathbf{x}, \mathbf{h}; \mathbf{x}', \mathbf{h}') = \sum_{\omega} \sum_{\mathbf{x}_s} \mathbf{G}'(\mathbf{x} + \mathbf{h}, \mathbf{x}_s; \omega) \mathbf{G}'(\mathbf{x}' + \mathbf{h}', \mathbf{x}_s; \omega) \sum_{\mathbf{x}_r} \mathbf{G}'(\mathbf{x} - \mathbf{h}, \mathbf{x}_r; \omega) \mathbf{G}'(\mathbf{x}' - \mathbf{h}', \mathbf{x}_r; \omega).$$

The next subsection shows how to use the subsurface-offset domain Hessian to compute the angle Hessian following the Fomel (2004) approach.

Angle-domain Hessian

Fomel (2004) define an image space transformation from subsurface offset to reflection and azimuth angle as:

$$\mathbf{m}(\mathbf{x}, \Theta) = \mathbf{T}'(\Theta, \mathbf{h})\mathbf{m}(\mathbf{x}, \mathbf{h}), \quad (4)$$

where $\Theta = (\theta, \alpha)$ are the reflection and the azimuth angles, and $\mathbf{T}'(\Theta, \mathbf{h})$ is the adjoint of the angle-to-offset transformation operator (slant stack).

Substituting the prestack migration image (subsurface offset domain) in equation 1 into equation 4 we obtain the expression for the prestack migration image in the angle-domain that follows:

$$\mathbf{m}(\mathbf{x}, \Theta) = \mathbf{T}'(\Theta, \mathbf{h})\mathbf{L}'\mathbf{d}(\mathbf{x}_s, \mathbf{x}_r; \omega), \quad (5)$$

The synthetic data can be modeled (as the adjoint of equation 5) by the chain of linear operator \mathbf{L} and the angle-to-offset transformation operator acting on the model space,

$$\mathbf{d}(\mathbf{x}_s, \mathbf{x}_r; \omega) = \mathbf{L}\mathbf{T}(\Theta, \mathbf{h})\mathbf{m}(\mathbf{x}, \Theta), \quad (6)$$

and its second derivative with respect to the model parameters $\mathbf{m}(\mathbf{x}, \Theta)$ and $\mathbf{m}(\mathbf{x}', \Theta')$ is the angle-domain Hessian

$$\mathbf{H}(\mathbf{x}, \Theta; \mathbf{x}', \Theta') = \mathbf{T}'(\Theta, \mathbf{h})\mathbf{H}(\mathbf{x}, \mathbf{h}; \mathbf{x}', \mathbf{h}')\mathbf{T}(\Theta', \mathbf{h}'). \quad (7)$$

NUMERICAL RESULTS

The TRIP synthetic dataset was created from a model with a constant-reflectivity flat reflector lying beneath a Gaussian low velocity anomaly (Figure 1). The data was modeled with the following acquisition geometry: the shots and receivers were positioned every 10 m on the interval $\mathbf{x} = [-2.0, 2.0]$ km. We also show rays from the shot position $x = 1$ km, to stress the point that the Gaussian anomaly produces an irregular angle of incidence of waves over the flat reflector (also an irregular sampling of the emergence angles at the surface).

Figures 2 and 3 show the subsurface-offset domain migration and the corresponding angle-domain migration. Notice the different patterns created by the uneven illumination in offset and angle. The subsurface offset is a less intuitive domain than the reflection angle. From Figure 2 it is difficult to interpret at which angles was the reflector illuminated while from Figure 3 it is obvious. At the center of the acquisition the reflector is illuminated from 0° to 45° . The corner of the reflector is only illuminated at small reflection angles. But in between, due to the low velocity anomaly, there are angles where there is no image.

Figures 4 and 5 show the subsurface-offset domain Hessian (15×15 coefficients filter). The first (Figure 4) shows the diagonal terms. The second (Figure 5) shows the Hessian off-diagonal terms at four different model space positions. From Figure 5a to Figure 5d the

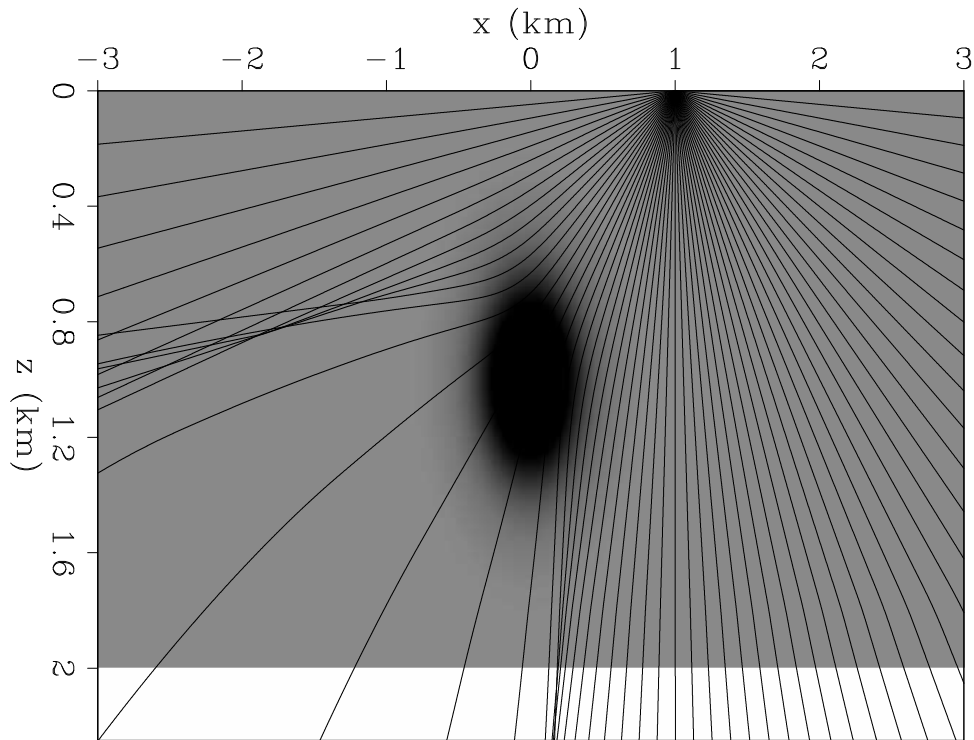


Figure 1: Gaussian anomaly velocity model with overlay rays showing the uneven illumination of the reflector. `alejandrol-rays` [CR]

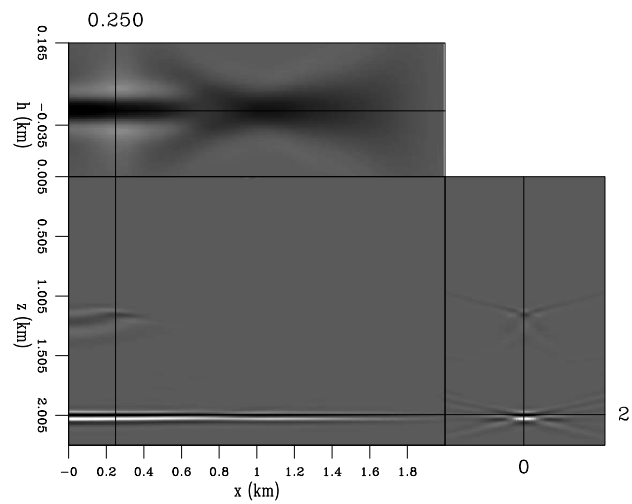


Figure 2: Shot-profile migration image in the subsurface-offset domain. `alejandrol-mig_off` [CR]

Figure 3: Shot-profile migration image in the angle domain
[alejandrol-mig_ang](#) [CR]

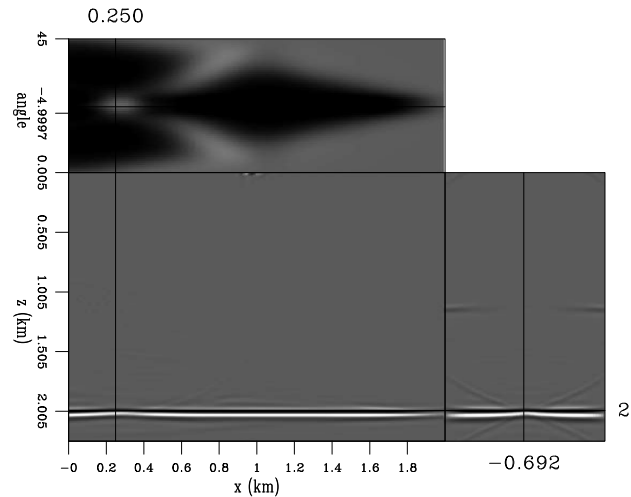
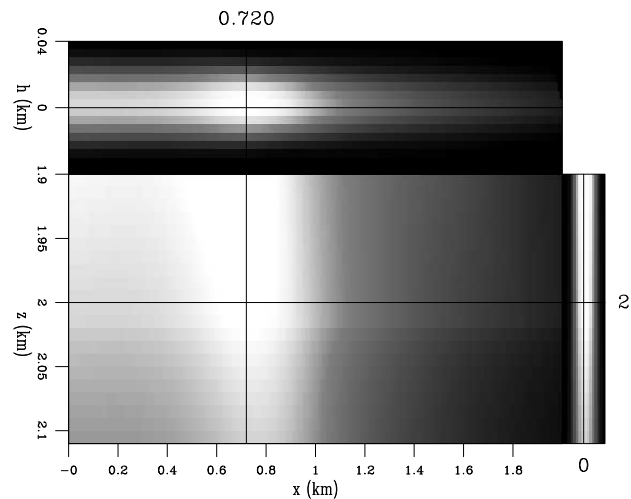


Figure 4: Diagonal of the subsurface-offset domain Hessian.
[alejandrol-illu_off16](#) [CR]



coordinates go from $\mathbf{x}_1 = (2.0, 0.)$, at the center of the acquisition, to $\mathbf{x}_4 = (2.0, 1.5)$, at the corner of the acquisition.

From Figure 4 we could interpret that the reflector has the maximum illumination at $x = 0.72$ km position, but from Figure 5c we can see that the filter shape is tilted (differently than Figure 5a). No more conclusions seems obvious from this Figures rather than there is information hidden in the off-diagonal terms of the subsurface-offset domain Hessian.

Figures 6 and 7 show the angle Hessian (15×15 coefficients filter). The first (Figure 6) shows the diagonal terms. The second (Figure 7) shows the Hessian off-diagonal terms at four different model space positions. From Figure 7a to Figure 7d the coordinates go from $\mathbf{x}_1 = (2.0, 0.)$, at the center of the acquisition, to $\mathbf{x}_4 = (2.0, 1.5)$, at the corner of the acquisition.

The diagonal of the angle Hessian looks similar to the diagonal of the subsurface-offset domain Hessian. But the "filter coefficients" look different. The angle dimension lacks of resolution to be able to interpret which angles get more illumination. The interpretation and improvement of resolution of the angle Hessian are topics of future research.

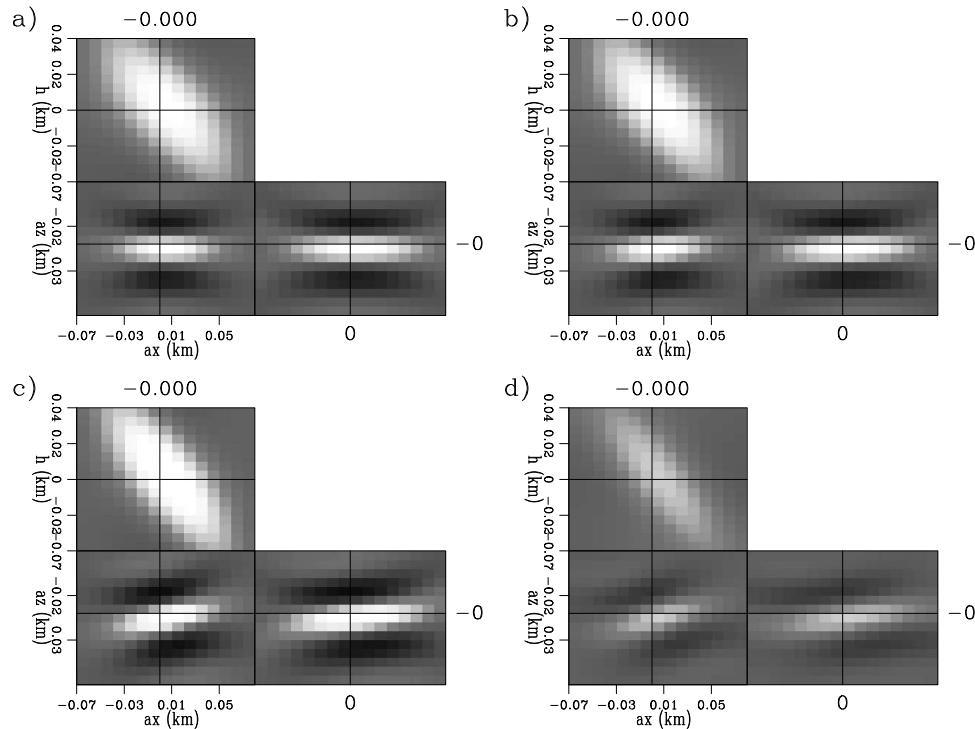


Figure 5: Subsurface-offset Hessian matrix off-diagonal elements for four different x positions a) $x = 0$ km, b) $x = 0.25$ km, c) $x = 0.72$ km, and d) $x = 1.5$ km. alejandro1-filt_off16 [CR,M]

CONCLUSIONS AND FUTURE RESEARCH

The wave-equation angle-domain Hessian can be computed from the subsurface offset wave-equation Hessian via an angle-to-offset transformation following the approach presented by Fomel (2004).

The Hessian computation in a model with a single reflector under a Gaussian velocity anomaly shows that the angle dimension lacks of resolution to be able to interpret which angles get more illumination. The interpretation and improvement of resolution of the angle Hessian topics of future research.

REFERENCES

- Chavent, G. and R. E. Plessix, 1999, An optimal true-amplitude least-squares prestack depth-migration operator: *Geophysics*, **64**, no. 2, 508–515.
- Claerbout, J. F., 1992, *Earth soundings analysis, processing versus inversion*: Blackwell Scientific Publications.

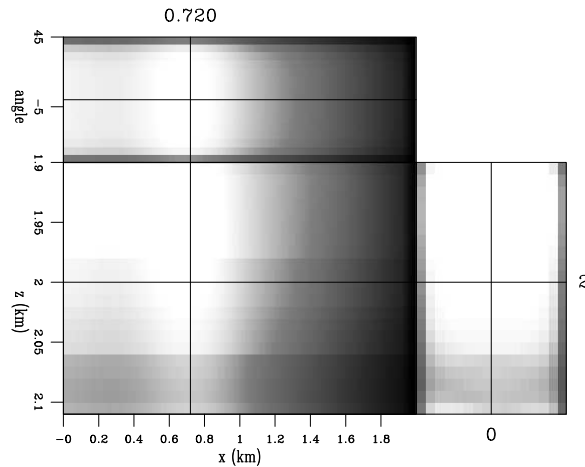


Figure 6: Diagonal of the angle Hessian. [alejandro1-illu_ang16](#) [CR]

Duquet, B. and K. J. Marfurt, 1999, Filtering coherent noise during prestack depth migration: *Geophysics*, **64**, no. 4, 1054–1066.

Fomel, S., 2004, Theory of 3-d angle gathers in wave-equation imaging: *SEG Technical Program Expanded Abstracts*, **23**, no. 1, 1053–1056.

Kuehl, H. and M. Sacchi, 2001, Generalized least-squares DSR migration using a common angle imaging condition: *Soc. of Expl. Geophys.*, 71st Ann. Internat. Mtg, 1025–1028.

Nemeth, T., C. Wu, and G. T. Schuster, 1999, Least-squares migration of incomplete reflection data: *Geophysics*, **64**, no. 1, 208–221.

Prucha, M. L., R. G. Clapp, and B. Biondi, 2000, Seismic image regularization in the reflection angle domain: *SEP-103*, 109–119.

Ronen, S. and C. L. Liner, 2000, Least-squares DMO and migration: *Geophysics*, **65**, no. 5, 1364–1371.

Sava, P. and S. Fomel, 2003, Angle-domain common-image gathers by wavefield continuation methods: *Geophysics*, **68**, 1065–1074.

Tarantola, A., 1987, *Inverse problem theory*: Elsevier.

Valenciano, A. A. and B. Biondi, 2004, Target-oriented computation of the wave-equation imaging Hessian: *SEP-117*, 63–76.

Valenciano, A. A. and B. Biondi, 2005, Wave-equation angle-domain hessian: *SEP-123*.

Valenciano, A. A., B. Biondi, and A. Guitton, 2005a, Target-oriented wave-equation inversion: Sigsbee model: *SEP-123*.

Valenciano, A. A., B. Biondi, and A. Guitton, 2005b, Target-oriented wave-equation inversion: *SEP-120*, 23–40.

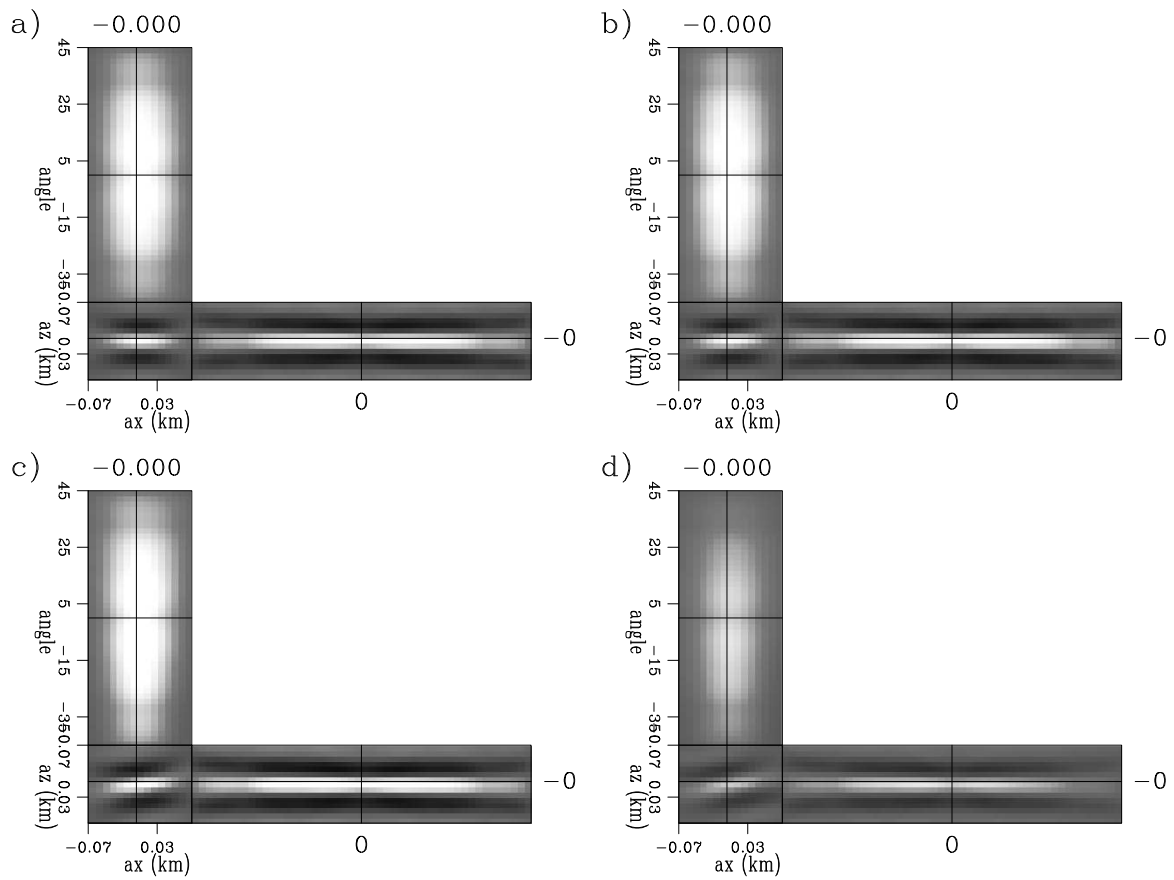


Figure 7: Angle Hessian matrix off-diagonal elements for four different x positions a) $x = 0$ km, b) $x = 0.25$ km, c) $x = 0.72$ km, and d) $x = 1.5$ km. [alejandro1-filt_ang48](#) [CR,M]

